Eur. Phys. J. D **27**, 215–221 (2003)
DOI: 10.1140/epjd/e2003-00276-4

THE EUROPEAN PHYSICAL JOURNAL D

Angular distributions for photo-double-ionization of the He isoelectronic sequence

S. Otranto[1,2,a] and C.R. Garibotti[1]

[1] CONICET and Centro Atómico Bariloche, 8400 S. C. de Bariloche, Argentina
[2] Departamento de Física, Universidad Nacional del Sur, 8000 Bahía Blanca, Argentina

Received 8 April 2003 / Received in final form 14 July 2003
Published online 16 September 2003 –

Abstract. We describe the three-body final state resulting from the photo-double-ionization (PDI) of two-electron ionic atoms by a modified C3 wave, denoted SC3. This continuum wave function accounts for the nuclear dynamical screening in the inter-electronic motion. We analyze the scaling properties of the triply differential cross-sections (TDCS). For an easier comparison with possible experimental results we analyze the correlation factor in the Gaussian parametrization of the TDCS, for different nuclear charges. We determine the dependence of the half width at half maximum of the Gaussian with the nuclear charge and discuss possible physical mechanisms.

PACS. 32.80.Fb Photoionization of atoms and ions

1 Introduction

Photo-double-ionization (PDI) of atomic systems is a showcase for the investigation of two electron dynamics in a system of three interacting Coulomb particles. Initial atomic states are not distorted by the incident photon and could be specified with high precision. This highlights the role of the final two electrons state and provides a severe test for any new model propose to describe the three particles continuum. A description of recent experimental and theoretical work for He targets can be found in two recent reviews [1,2].

The inclusion of the electron-electron correlation in the three body continuum state has been found to be essential for a realistic description of the PDI angular distributions [3–6]. In these works, use of some available analytical models of the final state showed that unphysical results were obtained when the interelectronic interaction was neglected. These models consider the continuum motion of the three particles as decoupled, and the wave function is expressed as a product of two-body Coulomb functions. Comparison of the C2 model, that only considers the electrons subject to the nuclear central field, with the C3 model [7], which describes the interelectronic interaction by incorporating an electron-electron Coulomb wave, clearly reveals the importance of the repulsion correlation for an appropriate description of the angular distributions in the PDI process [3,4]. The C3 model describes the electronic repulsion but neglects the non-orthogonal kinetic energy correlation [8]. This kinetic correlation could be partially considered by introducing effective Sommerfeld parameters, depending on the coordinates and momentums [9–12], or by multivariable hypergeometic waves [13].

These analytical approaches give a reasonable description of the shape of the angular distributions. However, they show disagreement between the PDI cross-sections resulting from the use of the three electromagnetic gauges representative of the photon-atom interaction. Besides, for He target the magnitude of the TDCS evaluated with these methods differs from the available experimental data [11].

In the last few years, intensive computational procedures have been introduced, showing good agreement with experiments. These are the convergent close coupling (CCC) method [14], the time-dependent close coupling calculation [15] and the *ab initio* hyperespherical R-matrix method with semiclassical outgoing waves [16]. These methods show good agreement with the experimental data and between gauges. A group theoretical approach has also been proposed to obtain the final continuum wave function extrapolating correlation-symmetries of doubly excited states, but up to the moment it has not been sufficiently tested experimentally [17]. A numerical solution of the three-body equation has also been recently obtained by using an exceptionally large computing power, and introducing complex coordinates to deal with the asymptotic behavior [18].

In a former paper, we proposed a modified version of the C3 model by performing a dilatation of the interelectronic coordinate through an energy dependent multiplicative factor, and we denoted this three-body state as SC3 [19]. That factor is meant to simulate the nuclear screening action on the electron-electron interaction, and was determined in order to correct the exponential

[a] e-mail: sotranto@uns.edu.ar

decrease of the total cross-sections magnitude as energy approaches threshold, typical of the C3 model. We have calculated TDCSs for photon impact on He, and we found agreement in shape between the velocity and length gauges, and with experimental data when the emitted electrons equally share the exceeding energy of the photon. However, discrepancies remain for other energy sharing cases. Furthermore, the SC3 model gives a much better description than the C3 approach of the total cross-section in the intermediate energy region.

In this paper we apply the SC3 method to the PDI of two-electron atomic ions in the ground state, *i.e.*: ions in the He isoelectronic sequence. We analyze the role the nuclear charge plays and how it weakens the electron-electron correlation effects. Pioneering work on this problem has been carried out by Kornberg and Miraglia, using the C2 and C3 wave function for the final three-body state [20]. They introduced a scaling law for the total, simple and triply differential cross-sections, and verified the scaling for the total and energy differential cross-sections. As usual in C3 theories, they found large differences between the results from the velocity and length gauges. The theoretical and experimental work about PDI of ions targets is limited, and mostly deals with the negative ion of hydrogen H^-. This is a theoretically difficult ion to deal with, because the electrons are in a loosely bound initial state with very strong correlation. Recently Kheifets and Bray using the CCC [21], and van der Hart and Feng [22] using a B-spline based technique, have evaluated the ratio of double to single photoionization cross-sections and the total PDI cross-sections for diverse atomic ions. They have confirmed the scaling rule proposed by Kornberg and Miraglia for total cross-sections. Furthermore, from the CCC results it could be inferred that disagreement between gauges for the PDI total cross-section of H^- is even found when a sophisticated 20-parameters Hylleras wave function for the initial state is used.

For targets with two electrons in the ground state the emission electronic angular distributions present a symmetry that is determined by the angular momentum of the photon. This leads to selection rules that forbid emission along some particular configurations of electrons momenta [23]. For linearly polarized photons, the TDCS can be factorized as a term that describes the electron-photon interaction times a Gaussian factor that takes account for the inter-electronic correlation [24]. This factor has been denoted the "Correlation Factor" and is supposed to depend on the emission energy and relative angle between electrons. The Gaussian form for this factor was proposed on the base of the Wannier theory, with a width dependent on the excess energy shared between the emitted electrons [25]. Nowadays, the Gaussian shape for the correlation factor is of standard use, with its full width at half maximum considered as an empirical parameter. This parametrization has been extended for arbitrary energy sharing and is valid for a wide range of excess energies E_f [26]. Here we evaluate this factor with the SC3 method and examine the dependence of the width on the charge of the target.

The scheme of the papers is the following: in Section 2 we briefly discuss the SC3 model and the wave functions used to represent the initial bound states, in Section 3 we present the TDCS for PDI of He-like atoms, in Section 4 we evaluate and discuss the interelectronic correlation factor, and in Section 5 conclusions are drawn.

2 Theory

As we have already mentioned above, the SC3 approximation gives equivalent angular distributions in the velocity and length gauges for equal-energy sharing emission [19]. In this regime, main difference between these two gauges amounts to an angle independent scaling factor. For unequal energy the method shows discrepancies between that gauges, which probably are a consequence of the sensitivity of the length gauge dipole amplitude to large distances, where the initial state may give a poor description which is enhanced by the oscillating nature of the final state. The introduction of more elaborated initial states is now being in course, but implies significant rewriting of our codes. Therefore here we present our results in the velocity gauge.

The TDCS for absorption of a photon of energy ω and emission of two electrons with momenta $\mathbf{k}_1, \mathbf{k}_2$ is given by:

$$\frac{\mathrm{d}\sigma}{\mathrm{d}\Omega_1 \mathrm{d}\Omega_2 \mathrm{d}E_1} = 4\pi^2 \alpha \, \frac{k_1 k_2}{\omega} |\langle \Psi_f | \widehat{\boldsymbol{\varepsilon}} \cdot (\boldsymbol{\nabla}_a + \boldsymbol{\nabla}_b) | \Psi_i \rangle|^2 \quad (1)$$

where α is the fine-structure constant. The photon energy ω, is distributed between the atomic ionization energy and the excess energy $E_f = E_1 + E_2$ where $E_1 = k_1^2/2$ and $E_2 = k_2^2/2$, are the energies of the emitted electrons. We consider the axis x as that of the incident linearly polarized photon, and z the corresponding to the polarization vector $\widehat{\boldsymbol{\varepsilon}}$. One of the electrons is emitted in the yz-plane with angle θ_2 relative to z. The direction of the other is determined by the angles ϕ_1, relative to the yz-plane, and θ_1 relative to $\widehat{\boldsymbol{\varepsilon}}$.

In the SC3 approximation [19] the final wave function is given by

$$\Psi_{SC3}(\mathbf{k}_1, \mathbf{k}_2, \mathbf{r}_1, \mathbf{r}_2) = N_f \, \mathrm{e}^{\mathrm{i}\mathbf{k}_1 \cdot \mathbf{r}_1 + \mathrm{i}\mathbf{k}_2 \cdot \mathbf{r}_2} \, {}_1F_1[\mathrm{i}a_1, 1, x_1] \times {}_1F_1[\mathrm{i}a_2, 1, x_2] \, {}_1F_1[\mathrm{i}a_3, 1, \beta\, x_3] \quad (2)$$

where $a_i = Z_i \mu_i / k_i$ are the Sommerfeld parameters, $x_i = -\mathrm{i}k_i \xi_i$ and $\xi_i = r_i + \widehat{\mathbf{k}}_i \cdot \mathbf{r}_i, i = 1, 2, 3$. Here, Z_i, μ_i, ξ_i and k_i indicate charges, reduced masses, coordinates and momentum of each electron relative to nucleus and between the electrons, respectively. The ${}_1F_1[a, b, x]$ is the Kummer function and the normalization constant N_f is obtained by requiring the wave function to have outgoing unitary flux:

$$N_f = \frac{1}{(2\pi)^3} \prod_{j=1}^{3} \mathrm{e}^{-a_j \frac{\pi}{2}} \Gamma(1 - \mathrm{i}a_j). \quad (3)$$

The dilatation parameter β in the interelectronic coordinate was determined in order to improve the threshold behavior of the total cross-section. We showed that,

Table 1. Variational parameters and ground state energies calculated using the wave function given in equation (6).

atom	a	b	λ	C_0	$\langle E\rangle$	$\langle E\rangle_{\rm exact}$
H^-	0.4666	1.0721	0.0373	–0.9307	–0.5259	–0.5277
He	1.4126	2.2068	0.1990	–0.6649	–2.9019	–2.9037
Li^+	2.3328	3.3006	0.3911	–0.4951	–7.2780	–7.2799
Be^{2+}	3.2614	4.3781	0.5892	–0.3918	–13.6536	–13.6555
B^{3+}	4.1973	5.4456	0.7896	–0.3236	–22.0290	–22.0309
C^{4+}	5.1387	6.5064	0.9911	–0.2754	–32.4043	–32.4062
N^{5+}	6.0846	7.5620	1.1932	–0.2396	–44.7795	–44.7814
O^{6+}	7.0341	8.6137	1.3957	–0.2120	–59.1546	–59.1565
F^{7+}	9.6622	7.9865	1.5984	–0.1901	–75.5297	–75.5317
Ne^{8+}	10.7079	8.9414	1.8013	–0.1723	–93.9048	–93.9068

resigning the Kato cusp condition when $x_3 \to 0$ [27], the introduction of this parameter corrects the exponential decay of the C3 approximation, for low excess energy. For He target, we found that this parameter is energy dependent, and proposed:

$$\beta = \frac{1}{\sqrt{E_f}}. \tag{4}$$

To consider highly charged nucleus we must scale the β. With this scope we consider the Hamiltonian for a two electron system in the field of a nucleus with charge Z_T and infinite mass. When we scale the electron coordinates $\mathbf{r}_1 \to \mathbf{r}_1/Z_T$, $\mathbf{r}_2 \to \mathbf{r}_2/Z_T$ the Schrödinger equation reduces to that for two electrons in a single-charged nucleus, repulsive $e{-}e$ interaction $1/Z_T r_{12}$ and energy E_f/Z_T^2. This shows that the relevance of potential electron correlation must decrease as the nuclear charge rises, and the energy must be scaled with E_f/Z_T^2. Then it follows that an appropriate scaling is

$$\beta = \frac{Z_T}{2\sqrt{E_f}}. \tag{5}$$

For an helium atom this reduces to equation (4). We represent the initial bound state by a modified Bonham and Kohl GS2 correlated wave function [28]:

$$\Psi_{GS2} = N_i \left(\mathrm{e}^{-c_1 r_1 - c_2 r_2} + \mathrm{e}^{-c_2 r_1 - c_1 r_2}\right) \times \left(\mathrm{e}^{-z_c r_{12}} + C_0 \mathrm{e}^{-\lambda r_{12}}\right). \tag{6}$$

Here an additional parameter z_c has been introduced to avoid the use of arbitrary cut-off in the evaluation of the transition amplitude. From the Ritz variational procedure we evaluate the parameters and the energies given by this wave function for the He-isoelectronic sequence [29]. The values obtained are displayed in Table 1, for $z_c = 0.01$. This simple functional form allows for partial analytical calculation of the transition amplitude using Nordsieck-like integrals [4,13].

3 Angular distributions

In this section, we calculate the TDCS for PDI of ions of the He-isoelectronic sequence, in the ground state. We consider the dependence on the nuclear charge of the angular distribution of one of the electrons in the yz-plane, when the emission angle of the other electron is kept fixed.

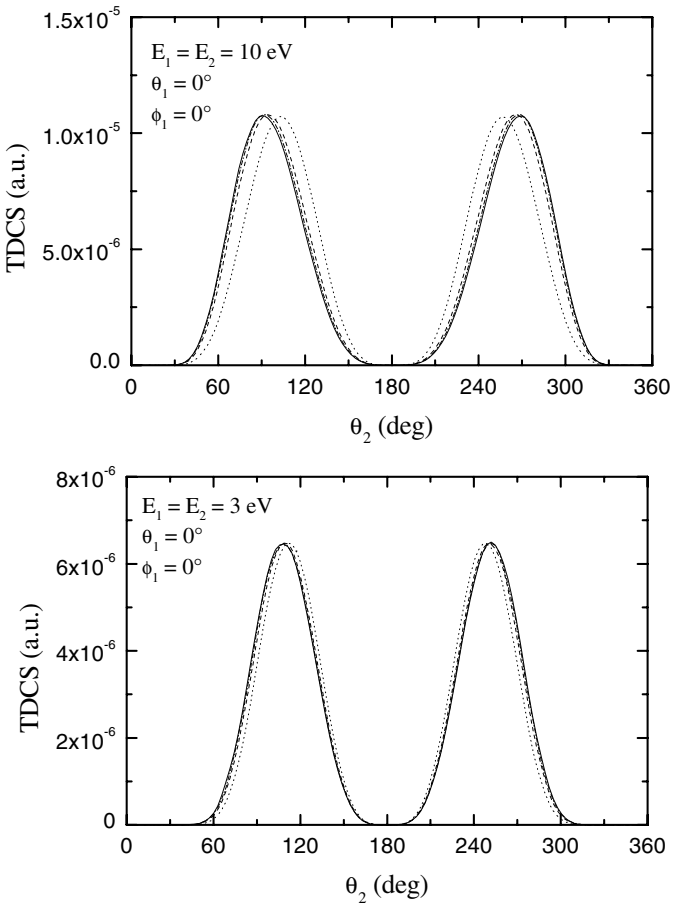

Fig. 1. TDCS for $E_f = 6$ eV and 20 eV for different core ions, when the electron 1 is emitted in the angle $\theta_1 = \phi_1 = 0°$. Theories: solid-line: O^{6+}; dot-dashed-line: C^{4+}; dashed-line: Be^{2+} ; dotted-line: He. All theories have been scaled to the He data.

In our figures, we observe the zeros associated to the selections rules [23]. In each case, the angular distributions for different ions have been normalized to the peak top value for the He target distribution.

In Figure 1 we present the TDCS for $E_f = 6$ eV and 20 eV, and equal energy sharing regime between the emitted electrons, for different core ions (He, Be^{2+}, C^{4+}, O^{6+}), when the electron 1 is emitted in the angle $\theta_1 = \phi_1 = 0°$. It could be seen that as the nuclear charge increases, the electrons tend to situate with an interelectronic angle θ_{12} close to $\pi/2$. This distribution is characteristic of a double electron emission reached after photon absorption by one electron followed by a binary collision with the remaining one. Once both electrons are emitted and leave the reaction zone they suffer a post-collisional focusing by action of the interelectronic repulsion, which tends to increment the angle θ_{12}. As could be seen from this figure, as the excess energy decreases the correlation effects are supposed to be more notorious and smaller variations in the angular distribution could be inferred for the different

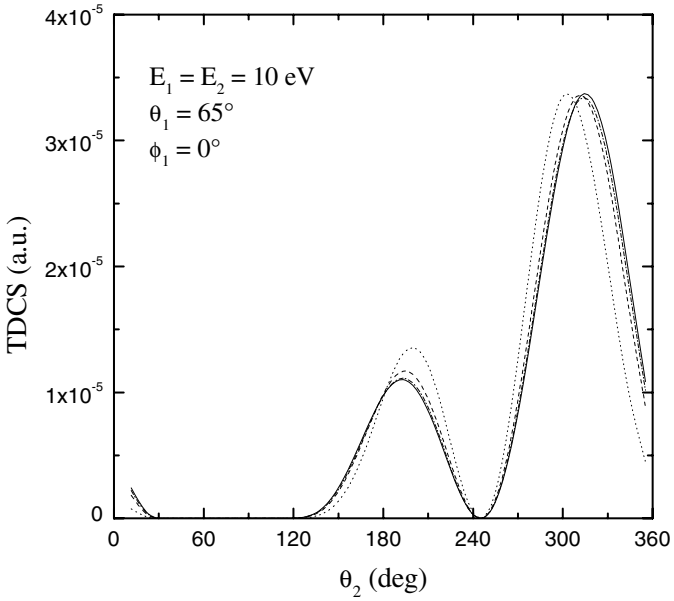

Fig. 2. TDCS for $E_f = 20$ eV, $\theta_1 = 65°$ and $\phi_1 = 0°$. Theories as in Figure 1.

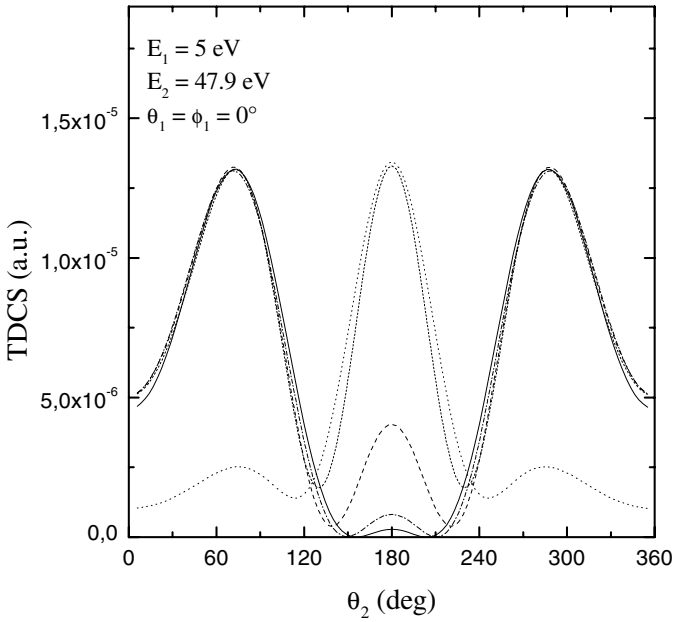

Fig. 3. TDCS for $E_f = 52.9$ eV, $\theta_1 = 0°$ and $\phi_1 = 0°$ in the unequal energy sharing regime ($E_1 = 5$ eV). Theories: solid-line: O^{6+}; dot-dashed-line: C^{4+}; dashed-line: Be^{2+}; short-dashed-line: Li^{+}; dotted-line: He. All theories have been scaled to the He data.

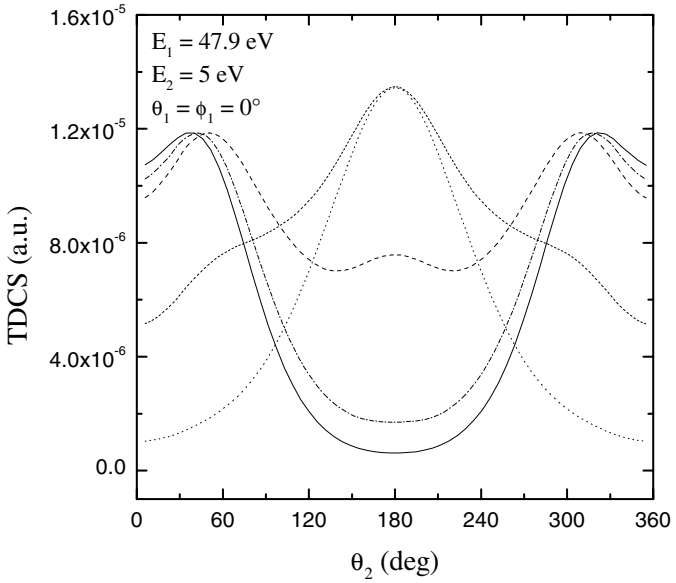

Fig. 4. TDCS for $E_f = 52.9$ eV, $\theta_1 = 0°$ and $\phi_1 = 0°$ in the unequal energy sharing regime ($E_1 = 47.9$ eV). Theories as in Figure 3.

ions when $E_f = 6$ eV. By the other side, for $E_f = 20$ eV these correlation effects are smaller and the peaks tend to situate closer to $\theta_{12} \approx \pi/2$.

The same trend could be observed from Figure 2, where $E_f = 20$ eV, $\theta_1 = 65°$ and $\phi_1 = 0°$. As Z_T increases the two electrons are emitted in quasi-orthogonal directions. We note that due to the photon field the altitude of the peaks become asymmetric, and the second electron is emitted preferentially towards the direction of the polarization vector.

In Figure 3 we show the TDCS for $E_f = 52.9$ eV, $\theta_1 = 0°$ and $\phi_1 = 0°$ in the unequal energy sharing regime. The slow electron energy is fixed ($E_1 = 5$ eV) and the fast electron angular distribution ($E_1 = 47.9$ eV) is analyzed. For He, the resulting distribution is known to reproduce with accuracy the experimental data [30]. As the Z_T increases, the relevance of the $e-e$ repulsion becomes relatively smaller, and it could be observed that the peak at 180° begins to disappear, leading to a two-peak structure.

In Figure 4 the slow electron distribution is presented for the same energy sharing as in Figure 3. Again, as the nuclear charge increases, the relevance of the repulsive $e-e$ interaction which pushes the electrons towards antiparallel directions decreases. As a result, this kind of "focusing" at 180° disappears and a two-peak structure remains.

In 1994, Kornberg and Miraglia proposed scaling laws for the total, simply differential and triply differential cross-section for PDI, derived in the frame of the C3 method when the highest $1/Z_T$ order is kept [20]. That scaling for the TDCS reads:

$$\frac{\mathrm{d}\sigma}{\mathrm{d}\Omega_1 \mathrm{d}\Omega_2 \mathrm{d}E_1}(Z_T, E) = \frac{1}{Z_T^6} \frac{\mathrm{d}\sigma}{\mathrm{d}\Omega_1 \mathrm{d}\Omega_2 \mathrm{d}\left(E_1/Z_T^2\right)} \left(1, E/Z_T^2\right). \tag{7}$$

Their scaling law for the total PDI cross-section has been confirmed even for low Z_T as was pointed out in the introduction. However, to our knowledge, results showing the validity of their scaling for the triply differential PDI cross-section have not been presented until now.

In Figure 5, we show the scaling properties of the TDCS of the present model as a function of the core charge, for $Z_T = 1, ..., 8$ when $E_f/Z_T^2 = 5$ eV and $\theta_1 = \phi_1 = 0°$. The figure is displayed in logarithmic scale to clearly appreciate the variation with Z_T. We note that,

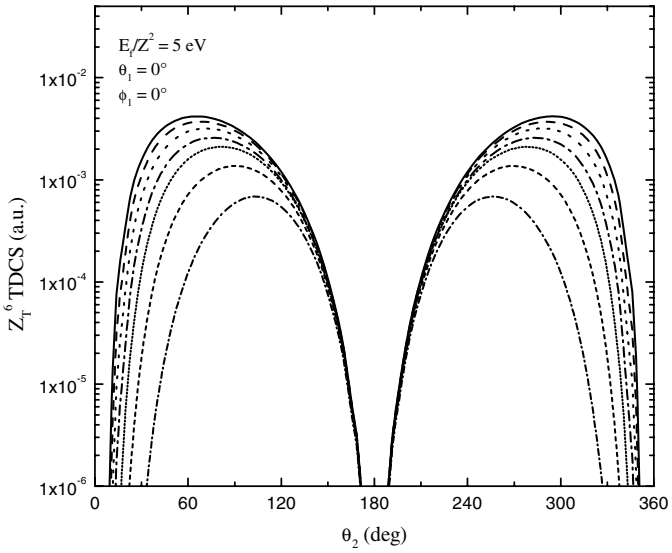

Fig. 5. Scaled TDCS, for $Z_T = 1, ..., 8$ when $E_f/Z_T^2 = 5$ eV and $\theta_1 = \phi_1 = 0°$. Theories: solid-line: O^{6+}; dashed-line: N^{5+}; dotted-line: C^{4+}; dot-dashed-line: B^{3+}; short-dotted-line: Be^{2+}; short-dashed-line: Li^{+}; short-dot-dashed-line: He.

as Z_T increases, the peak maximum of the angular distribution of electron 2 displaces towards the direction of the other electron, and the peak width in half maximum increases slightly. However there is not a "saturation" for the angular distribution. It could be seen, that for increasing nuclear charge, the angular distributions tend to the uncorrelated distribution $(1 + \cos\theta_2)^2$. The maximum of the two lobes goes to $\theta_1 = 0$ and the corresponding distributions approach the envelope. In this sense, our results show that the Kornberg and Miraglia scaling law for the TDCS is attained in the $Z_T \to \infty$ limit.

4 Electron-electron correlation factor

Huetz *et al.* [24], developed a Wannier theory for PDI of noble gases and realized that the TDCS could be expressed in the near threshold region and in equal energy sharing regime as follows,

$$\frac{\mathrm{d}\sigma}{\mathrm{d}\Omega_1 \mathrm{d}\Omega_2 \mathrm{d}E_1} = C(\theta_{12})(\cos\theta_1 + \cos\theta_2)^2 \qquad (8)$$

where $C(\theta_{12})$ is the usually called "correlation factor". It describes the electrons correlation, and the other angular factor accounts for the interaction of the photon with each electron. During the last few years, this parametrization of the TDCS has been widely used and, the Gaussian ansatz [25] has been usually employed to represent the correlation factor:

$$C_G(\theta_{12}) = A(E_f) \exp\left[-\frac{4\ln 2(\theta_{12} - 180°)^2}{\Gamma(E)^2}\right]. \qquad (9)$$

For He targets and low exceeding energies, the half-width at half maximum $\Gamma(E)$ shows a clear dependence with the excess energy given by: $\Gamma \sim E_f^{1/4}$ [25].

A simple interpretation can be given [1,26]. The electrons are initially in a very symmetric radial configuration, and their kinetic energies are well balanced meanwhile they are in the vicinity of the ion core. As they move out, the Coulomb repulsion drives the mutual angle between ejected electrons towards $\theta_{12} = \pi$, and stabilizes the angular correlations. The Wannier mechanism for the threshold ionization presumes that the electrons recede being at equal distances from the atomic core ($r_1 = r_2$) and in opposite directions ($\theta_{12} = \pi$). Meanwhile the nuclear attraction produces a "dynamical screening" which destabilizes the correlation between the escaping electrons, and in a naive approximation produces an angular motion around $\theta_{12} = \pi$. In the three-body interactions the only θ_{12} dependence is contained in the electron-electron repulsion term, that near the Wannier saddle can be expanded as:

$$|\mathbf{r}_1 - \mathbf{r}_2|^{-1} = \frac{1}{R\sqrt{1 - \cos\theta_{12}}} = \frac{1}{R\sqrt{2}} + \frac{(\pi - \theta_{12})^2}{8R\sqrt{2}} + \frac{5(\pi - \theta_{12})^4}{384R\sqrt{2}} + ... \qquad (10)$$

The R is the hyper-radius $\sqrt{r_1^2 + r_2^2}$, that at this point has a certain effective value $R = R_0$ [34]. Retaining terms up to second-order, the electrons move out performing an angular harmonic motion around the point $\theta_{12} = \pi$, with a frequency that depends on R_0. We can write an oscillator Hamiltonian H_θ for the electron-electron relative angular motion, with eigenfunction [25,33,34]:

$$\chi(\theta_{12}) = \mathrm{e}^{a(\pi - \theta_{12})^2}. \qquad (11)$$

The parameter a is associated to a Wannier radius R_0 as $a = 1/8R_0$, which also determines an angular $e{-}e$ oscillatory energy around $\theta_{12} = \pi$. This energy only depends on R_0, and is determined by the frequency of the oscillation produced by the nuclear action, and therefore it depends on the nuclear charge Z_T. The probability that the two electrons are emitted with a relative angle is given by $|\chi(\theta_{12})|^2$, that is the factor $C_G(\theta_{12})$ appearing in equation (9).

In the frame of the C3 approximation, Briggs and Schmidt [1] give another interpretation for the correlation factor. It is possible to expand the square modulus of the Coulomb factor associated with the electron-electron relative motion:

$$|N(k_{12})|^2 = \frac{\frac{2\pi}{k_{12}}}{\exp(\frac{2\pi}{k_{12}}) - 1}. \qquad (12)$$

For equal energy sharing and $k_{12} \to 0$, we have

$$|N(k_{12})|^2 \to \mathrm{e}^{-\frac{\pi}{\sqrt{E_f}} - \frac{\pi}{8\sqrt{E_f}}(\pi - \theta_{12})^2 - \frac{5\pi}{384\sqrt{E_f}}(\pi - \theta_{12})^4}. \qquad (13)$$

We note that this factor does not include the nuclear dynamical screening and it only contains a partial dependence of the transition amplitude on θ_{12}.

Nowadays, the $\Gamma(E)$ is usually treated as an empirical parameter and is determined from experimental

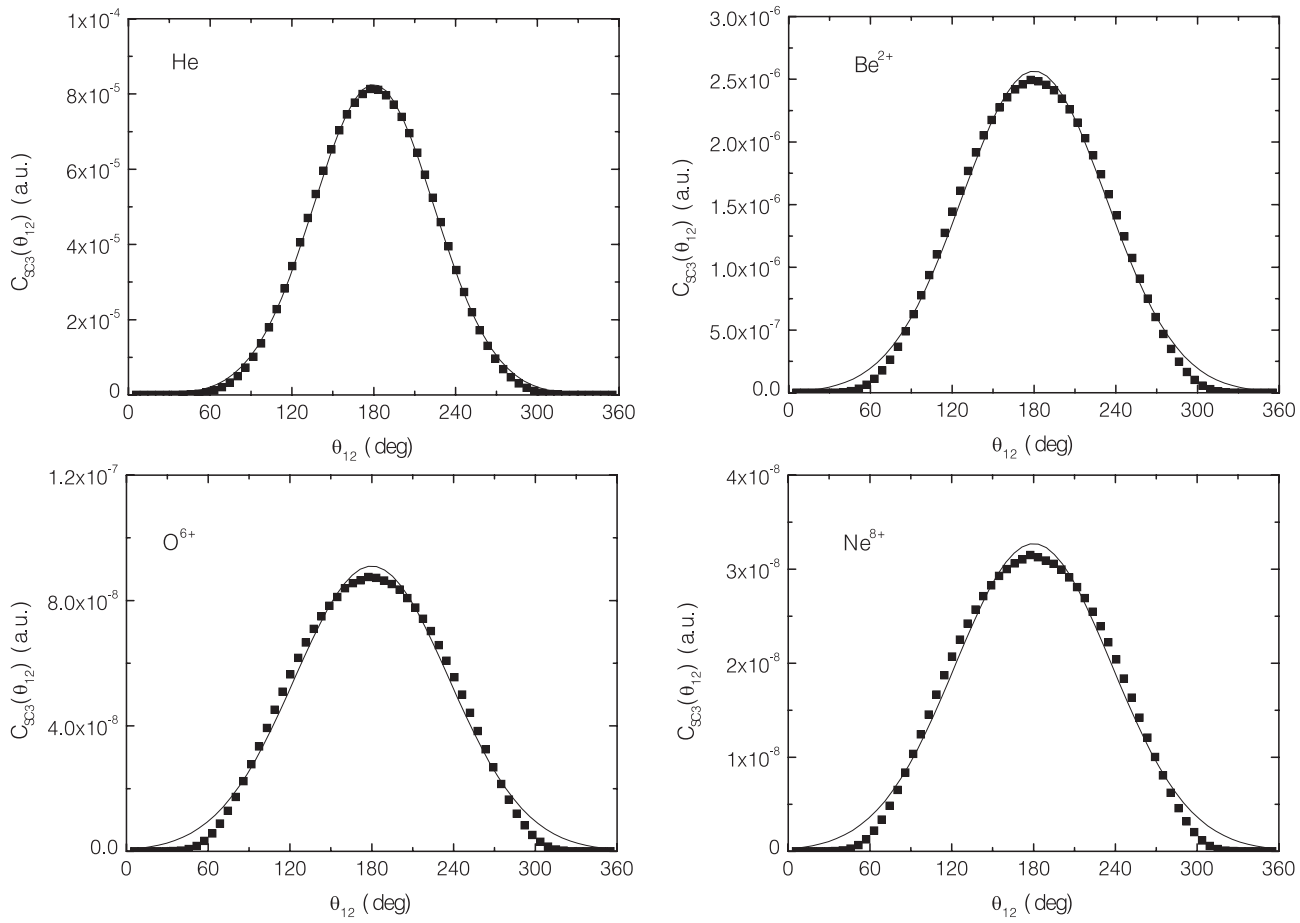

Fig. 6. Correlation coefficients $C_{SC3}(\theta_{12})$ for ions with core charge: $Z_T = 2, 4, 8, 10$. The excess energy considered is 20 eV. A Gaussian fit has also been included for comparison.

data and theories [1,26,31,32]. This parametrization valid for linearly polarized photons and equal sharing emission has been generalized for other polarizations and the unequal energy sharing regime [26]. Several authors [25,33], have claimed that this correlation factor should be θ_{12}-independent for $Z_T \geq 3$, while others debate this result and the accuracy of a strict Gaussian shape [34].

We have fitted the TDCS given by the SC3 theory with equation (8), for $E_1 = E_2 = 10$ eV and angles $\theta_1 = \phi_1 = 0°$. This gives the correlation coefficients $C_{SC3}(\theta_{12})$, that are presented in Figure 6 for ions with core charge: $Z_T = 2, 4, 8, 10$.

In Table 2 we tabulate our values for Γ, as a function of E_f, for $Z_T = 2, 4, 6, 8$ for energies $E_f = 6, 10, 20$ eV. We observe that the SC3 method gives a width that increases with energy and core charge. This is in agreement with results shown in Figure 1, and indicate a reduced relevance of the electron-electron correlation. For He, the resulting value could also be compared with the experimental value of Turri *et al.* [35], *i.e.*: 91 degrees at $E_f = 20$ eV.

The Gaussian form is in excellent agreement with the SC3 model predictions for the He case, but shows slight deviations when Z_T increases. The Gaussian ansatz implies that the electrons in the near threshold region would tend to situate as opposite as possible. However, for a highly charged nucleus, the dynamic screening now allows electrons to deviate from $\theta_{12} \approx \pi$ and probably $C(\theta_{12})$ should include terms of even-order higher than 2. Anyway, the SC3 model shows a clear dependence of $C(\theta_{12})$ with θ_{12} in contrast with the flat prediction of Rau.

Table 2. $\Gamma(E_f)$ values obtained from a Gaussian fit of $C_{SC3}(\theta_{12})$.

	E_f		
atom	6 eV	10 eV	20 eV
He	92.6(5)°	99.2(5)°	104.3(4)°
Be^{2+}	97.7(6)°	109.0(8)°	124(1)°
C^{4+}	99.3(6)°	112.0(9)°	130(1)°
O^{6+}	100.3(6)°	113.6(9)°	133(2)°
Ne^{8+}	100.8(6)°	114(1)°	134(2)°

We also studied possible deviations from equation (8). We included the anharmonic terms of equation (10) in the Hamiltonian H_θ and tried an ansatz for the corresponding eigenfunction:

$$\chi(\theta_{12}) = \mathrm{e}^{a(\pi-\theta_{12})^2 + b(\pi-\theta_{12})^4}. \quad (14)$$

We kept the relation $b = 5a/48$ given by the potential equation (10) and therefore a single parameter remained,

and is associated to the effective Wannier radius R_0, which determines the $e-e$ oscillatory energy. The probability that the two electrons are emitted with a relative angle is given by $|\chi(\theta_{12})|^2$ and gives an alternative form for the correlation factor. We used this "anharmonic" Gaussian form to fit the SC3 results, and we found slight differences with the former results, which would probably be experimentally unobservable. However the differences turned more noticeable as the nucleus charge and the excess energy were increased.

5 Conclusions

In this paper we have studied the TDCS for PDI of ions in the He isoelectronic sequence. We have represented the final continuum state using a recently introduced SC3 model, which has shown to give better results than the C3 model for He targets [19]. For equal energy sharing we have found that the two-electron interaction correlation effects diminish as the nuclear charge or the excess energy increases.

For unequal energy sharing, we clearly observe how the "focusing" at the relative angle 180° disappears as the interaction of the electron with the nucleus overcome the repulsive $e-e$ interaction.

We studied the Kornberg and Miraglia scaling law for the TDCS for $Z_T = 1, ..., 8$, and found that for low Z_T our results separate from their prediction, which becomes meaningful as the nuclear charge increases. Meanwhile the scaling law for the total cross-section, though developed in the high Z_T limit, has shown to be valid for low Z_T values also. Therefore, the present results show that the Kornberg and Miraglia scaling for the n-differential cross-section turns better as lower is n.

We fitted our results for the TDCS with the usual Gaussian parametrization for the correlation factor. We have found that for $Z_T \geq 3$, our results are well reproduced by the Gaussian ansatz, in disagreement with some existing Wannier-type models [25,33]. Furthermore we have evaluated and tabulated the empirical parameters $\Gamma(E_f)$ from our results for different ions and energies. Experiments or further theoretical analysis would be very helpful to elucidate on this point.

The present simple model for the final three-body wave function is able to describe the main physical features of the angular distributions in PDI process for multiply charged ions. Furthermore it shows the convenience and potential of an analytic wave approach to predict general rules such as the scaling laws.

We would like to acknowledge J.E. Miraglia for calling our attention in this problem and G. Gasaneo for continuous interest. This work has been supported by PICT 99/03/06249 and 98/03/04021 of the ANPCYT, and PGI 24/F027 of the UNS (Argentina).

References

1. J.S. Briggs, V. Schmidt, J. Phys. B: At. Mol. Opt. Phys. **33**, R1 (2000)
2. G. King, L. Avaldi, J. Phys. B: At. Mol. Opt. Phys. **33**, R215 (2000)
3. F. Maulbetsch, J.S. Briggs, J. Phys. B: At. Mol. Opt. Phys. **26**, L647 (1993)
4. M.A. Kornberg, J.E. Miraglia, Phys. Rev. A **48**, 3714 (1993)
5. M. Pont, R. Shakeshaft, Phys. Rev. A **51**, R2676 (1995)
6. D. Proulx, R. Shakeshaft, Phys. Rev. A **48**, R875 (1993)
7. C.R. Garibotti, J.E. Miraglia, Phys. Rev. A **21**, 572 (1980)
8. H. Klar, Z. Phys. D: At. Mol. Clust. **16**, 231 (1990)
9. J. Berakdar, J.S. Briggs, Phys. Rev. Lett. **72**, 3799 (1994)
10. J. Berakdar, Phys. Rev. A **53**, 2314 (1996).
11. S.P. Lucey, J. Rasch, C.T. Whelan, H.R.J. Walters, J. Phys. B: At. Mol. Opt. Phys. **31**, 1237 (1998)
12. M.A. Kornberg, V.D. Rodriguez, Eur. Phys. J. D **5**, 221 (1999)
13. F.D. Colavecchia, G. Gasaneo, C.R. Garibotti, J. Math. Phys. **38**, 6603 (1997)
14. A.S. Kheifets, I. Bray, Phys. Rev. A **54**, R995 (1996); J. Phys. B: At. Mol. Opt. Phys. **31**, L447 (1996)
15. J. Colgan, M.S. Pindzola, F. Robicheaux, J. Phys. B: At. Mol. Opt. Phys. **34**, L457 (2001)
16. L. Malegat, P. Selles, A.K. Kazansky, Phys. Rev. Lett. **85**, 4450 (2000)
17. Y. Qiu, J. Burgdörfer, Phys. Rev. A **59**, 2738 (1999)
18. T.M. Rescigno, M. Baertschy, W.A. Isaacs, C.W. McCurdy, Science **286**, 2474 (1999)
19. S. Otranto, C.R. Garibotti, Eur. Phys. J. D **21**, 285 (2002)
20. M.A. Kornberg, J.E. Miraglia, Phys. Rev. A **49**, 5120 (1994)
21. A.S. Kheifets, I. Bray, Phys. Rev. A **58**, 4501 (1998)
22. H.W. van der Hart, L. Feng, J. Phys. B: At. Mol. Opt. Phys. **34**, L601 (2001)
23. F. Maulbetsch, J.S. Briggs, J. Phys. B: At. Mol. Opt. Phys. **28**, 551 (1995)
24. A. Huetz, P. Selles, D. Waymel, J. Mazeau, J. Phys. B: At. Mol. Opt. Phys. **24**, 191 (1991)
25. A.R.P. Rau, J. Phys. B: At. Mol. Opt. Phys. **9**, L283 (1976)
26. S. Cvejanovic, T.J. Reddish, J. Phys. B: At. Mol. Opt. Phys. **33**, 4691 (2000)
27. T. Kato, Commun. Pure Appl. Math. **10**, 151 (1957)
28. R.A. Bonham, D.A. Kohl, J. Chem. Phys. **45**, 2471 (1966)
29. S. Otranto, C.R. Garibotti, G. Gasaneo, Nucl. Instr. Meth. B (submitted)
30. O. Schwarzkopf, B. Krässig, V. Schmidt, F. Maulbetsch, J.S. Briggs, J. Phys. B: At. Mol. Opt. Phys. **27**, L347 (1994)
31. A. Huetz, J. Mazeau, Phys. Rev. Lett. **8**, 530 (2000)
32. G. Turri, L. Avaldi, P. Bolognesi, R. Camilloni, M. Coreno, J. Berakdar, A.S. Kheifets, G. Stefani, Phys. Rev. A **65**, 034702 (2002)
33. J.M. Feagin, J. Phys. B: At. Mol. Opt. Phys. **17**, 2433 (1984)
34. A.K. Kazansky, V.N. Ostrovski, J. Phys. B: At. Mol. Opt. Phys. **26**, 2231 (1993)
35. G. Turri, L. Avaldi, P. Bolognesi, R. Camilloni, M. Coreno, J. Berakdar, A. Kheifets, G. Stefani, Phys. Rev. A **65**, 034702 (2002)